CHARACTERIZATION OF THE DIFFERENT FRACTIONS OBTAINED FROM THE PYROLYSIS OF ROPE INDUSTRY WASTE

Marta Andrade [1], José B. Parra [2], Marta Haro[2], Ana S. Mestre[1], Ana P. Carvalho[1*], Conchi O. Ania[2*]

[1]Departamento de Química e Bioquímica and CQB, Faculdade de Ciências da Universidade de Lisboa, Ed. C8, Campo Grande, 1740-16 Lisboa, Portugal
[2] Instituto Nacional del Carbon (INCAR, CSIC) 33011 Oviedo, Spain

[*]Corresponding authors: Telephone: +351 217500897; Fax: +351 217500088; E-mail: ana.carvalho@fc.ul.pt (Ana P. Carvalho); Telephone: +34 985119090; Fax: +34 985297662; E-mail: conchi.ania@incar.csic.es (Conchi O. Ania).

Abstract

A study of the possibilities of pyrolysis for recovering wastes of the rope's industry has been carried out. The pyrolysis of this lignocellulosic residue started at 250 ºC, with the main region of decomposition occurring at temperatures between 300 and 350 ºC. As the reaction temperature increased, the yields of pyrolyzed gas and oil increased, yielding 22 wt.% of a carbonaceous residue, 50 wt.% tars and a gas fraction at 800 ºC. The chemical composition and textural characterization of the chars obtained at various temperatures confirmed that even if most decomposition occurs at 400 ºC, there are some pyrolytic reactions still going on above 550 ºC. The different pyrolysis fractions were analyzed by GC-MS; the produced oil was rich in hydrocarbons and alcohols. On the other hand, the gas fraction is mainly composed of CO_2, CO and CH_4. Finally, the carbonaceous solid residue (char) displayed porous features, with a more developed porous structure as the pyrolysis temperature increased

Keywords

Sisal, Residues, Pyrolysis, Gas fraction, Oil fraction

1. INTRODUCTION

Sisal fiber is one of the most widely used natural fibers. It is obtained from the leaves of sisal (*Agave Sisalana*), an autoctone plant from Mexico, which is now also widely grown in tropical countries in Africa, the West Indies and the Far East [1].

Agave Sisalana belongs to the group of hard fibers which also includes flax, abaca, jute, coir and some others. Its annual production accounts for 2% of the overall worldwide production of natural fibers, which represents *ca*. 65% of the world's fibers. In 2008, the production of sisal fiber was around 250 thousands of tons, with Brazil, Tanzania and Kenya being currently the world's largest producers [2].

As for other lignocellulosic fibers, the major chemical constituents of sisal are cellulose and lignin, although large variations in the chemical composition can be found in the literature. As an example, Barreto *et al.* [3] reported the composition of natural sisal fibers from Brazil as 65.8% of cellulose, 12% of hemicelluloses, 9.9% of lignin, 0.8% of pectin and 0.3% of wax and water soluble compounds.

Sisal is one of the most widely used natural fibers, due to its outstanding characteristics related to its low cost and density, high specific resistance, good mechanical properties, and non-toxicity [1]. Recently, increasing interest has arisen towards exploring novel applications for sisal, namely as reinforcement of polymers, rubber, gypsum and cement matrices, creating a large range of technological applications. However, as it was for centuries, its main use nowadays is still as raw material for the rope industry.

The rope manufacture process produces quite a large amount of residues that are frequently either recycled for the production of low quality ropes or used as fuel. In this regard, the potential of this waste to be transformed in an added-value product beyond the fabrication of low quality ropes has been explored in different fields, covering for instance the pyrolytic degradation of the residues and the synthesis of adsorbents, namely carbon fibers [4-6] and activated carbons [7,8] that proved to be efficient adsorbents for the removal of pharmaceutical compounds from water. Moreover, rising worldwide concerns on environmental pollution have urged the development of new strategies as alternatives for the disposal of wastes complying with current environmental regulations. In this regard, pyrolysis has proven to be an effective technology for the valorisation of several types of

residues. Thus the purpose of this study was to investigate the pyrolysis behaviour of sisal fibers discarded from the rope industry, by analyzing the composition of the different fractions obtained as well as their potential applications in different fields.

2. EXPERIMENTAL SECTION

2.1. Sample

Sisal fibers discards were provided by a rope manufacturer in Portugal (Cordex). The as--received residue was cut into small pieces (*ca*. 1-2 cm) before any analysis, still preserving the characteristic morphology of sisal fibers.

2.2. Pyrolysis

The pyrolysis of the rope waste (*ca.* 20 grams in each run) was carried out in a quartz reactor placed in a tubular horizontal furnace. In order to ensure an inert environment during the experiments a 100 mL min^{-1} flow rate of nitrogen was continuously fluxed through the reactor. Different pyrolysis temperatures (400, 550, 700 and 800 °C) were investigated at constant heating rates (10 ºC min^{-1}). The volatiles evolved during the pyrolysis passed through various consecutive glass condensers immersed in ice salt cooling mixture (*ca.* -20 ºC) where the condensable liquid fraction was collected. The non-condensable gases were collected in 3 L Tedlar® bags (with a polypropylene fitting for sampling). Gas samples were collected at the following temperatures: 300, 400, 550, 700, 800 and 850 °C. Once the pyrolysis was over, the solid carbonaceous residue was recovered from inside the quartz reactor for subsequent characterizations. Carbonaceous residues were named C-T, where T stands for the final pyrolysis temperature. The solid and oil fraction yields were calculated from the weight of each fraction, while the gas yield was evaluated by difference.

The aqueous fraction recovered in the condensers (mostly water) accounted for ca. 10-15 wt.%, regardless the pyrolysis temperature. It was separated from the organic fraction by centrifugation and it was further discarded (not analysed as it was outside the scope of this paper).

2.3. Analysis

The organic fraction obtained upon pirolysis was dried, using anhydrous sodium sulphate, filtered and dissolved in dichloromethane for further analysis by GC-MS, using an Agilent 7890A gas chromatograph coupled to an Agilent 5975C quadrupole detector. The gas chromatograph was equipped with a 30 m x 0.25 mm capillary column coated with a 0.25 mm thick film of 5% phenylmethylpolysiloxane (HP-5). Helium of 99.999% purity was employed as a carrier gas at a constant flow rate of 1.8 mL min-1. The initial oven temperature of 40 ºC was held for 10 min. The oven was programmed from 40 to 300 ºC at 8 ºC min-1 and the maximum temperature was maintained for 30 min, and a splitting ratio of 1:50 was used. The detector and injector temperature were 350 and 300 °C, respectively, and the volume of sample injected was 1 μL. Data were collected in the full-scan mode between m/z 33-533. The compounds in the oil fraction were identified by comparison with those reported in the literature [9-12] and in the Wiley and NIST computer libraries. Although quantification of the components in the oil fraction was not possible due to the large number of compounds and functionalities present in the chromatographied fraction, a semiquantitive analysis was performed. The relative amount of the detected compounds was evaluated by calculating the area (%) from the total chromatographied area.

The gases were analyzed in a Hewlett-Packard HP 6890 gas chromatograph fitted to a thermal conductivity detector (TCD) and two packed columns (HP 10FT Porapak N, 80/100 and HP 3FT Molecular Sieve 13×, 45/60). The oven temperature was set at 50 ºC and the carrier gas flow rate (He) was 20 mL min^{-1}. The injector and detector temperatures were 80 and 220 ºC, respectively. The TCD was calibrated with a standard gas mixture at periodic intervals.

Chemical characterization of the solid fraction included: proximate analysis and elemental analysis (using a LECO CHN-2000 apparatus for the determination of the C, H and N content, a LECO S-144DR for the S content, and a LECO VTF-900 for the oxygen content).

The solid fraction was further characterized by gas adsorption of CO_2 at 0 ºC, using an automatic Tristar 3020 apparatus from Micromeritics. Before the experiments, the samples

were outgassed under vacuum at 120 °C overnight. The isotherms were used to calculate the specific surface area S_{BET}, total pore volume V_T, and pore size distribution using the density functional theory (DFT) method [13].

The as-received rope waste and the solid carbonaceous residue after pyrolysis were also characterized by thermal analysis. The thermal analyzer (Labsys, Setaram) was set to operate at a heating rate 15 ºC min^{-1} under a nitrogen flow rate of 100 mL min^{-1}. For each measurement about 25 mg of sample was used.

3. RESULTS AND DISCUSSION

3.1. Characterization and thermal behaviour of the as-received waste in a thermobalance

Table 1 shows some bulk characteristics of the as-received rope residues. The lignocellulosic character of this material was confirmed by the large oxygen content determined by elemental analysis and the X-ray diffraction patterns (Figure 1A). The diffractograms showed the typical diffraction peaks of the crystal polymorph of cellulose I (characteristic peaks at 2θ = 16.3 and 22.5º) associated to the (101) and (002) planes of the native crystal structure of cellulose [14,15]. This crystal form arises from the hydrogen bonds between cellulose molecules arranged in a regular and ordered system. This is in good agreement with the fact that sisal is a cellulose-rich fiber as above-mentioned.

Investigating the thermal stability of natural fibers is important to evaluate their potential use in the processing of biomaterials [16]. For this reason, the thermal degradation of sisal was initially studied by thermal analysis at different heating rates (Figure 1B). The thermograms showed that the decomposition takes place in a narrow temperature range, with a first weight loss occurring at approximately 100 ºC (*ca.* 6-7 %) and a main devolatization step detected at temperatures between 250-350 ºC. The first peak was attributed to the loss of moisture, what is a common feature observed for lignocellulose fibers [17,18]. The values of water loss obtained by thermal analysis are in agreement with the moisture content evaluated from ultimate analysis.

Table 1

Figure 1

The pyrolytic reaction started at temperatures above 250 ºC, and the rate of decomposition (DTG) curves showed two distinct peaks at 300 and 350 ºC, indicating that the decomposition of the rope wastes occurs in two steps. The weight loss at about 300 ºC is a shoulder in the main peak, due to depolymerization of hemicelluloses and the cleavage of glucosidic linkages of cellulose [19]. The mass loss occurring at 350 ºC is assigned to the decomposition of cellulose oligomers into tars (levoglucosan and low molecular mass volatile compounds like aldehydes, ketones or furans [20]. The rupture of α- and β-aryl-alkyl-ether linkages originated from the thermal breakdown of lignin might also contribute to the mass loss behavior of these fibers [18]. In general terms, the thermal degradation of the rope wastes followed a similar trend than that of raw sisal fibers [21]. A gradual thermal degradation of the fibers was still observed at higher temperatures (*ca.* above 400 ºC), which is attributed to the decomposition of cyclic rings and/or further carbonization of the formed tars [18]. Indeed, the char residue varied from 30 to 21 wt.% at 400 and 800 ºC, respectively.

From the thermal profiles under inert atmosphere at different heating rates, the activation energies of the two decomposition processes detected during pyrolysis were calculated. The obtained values were 88 and 137 kJ mol^{-1}, which are slightly lower than the values reported for pure sisal fibers [22], but correlate very well with those of other lignocellulosic materials [18].

3.2. Pyrolysis yields

After investigating the thermal behaviour of the sisal-based residues in a thermobalance, pyrolysis experiments were carried out at several temperatures: 400, 550, 700 and 800 ºC. The solid, liquid and gas yields (wt.%) obtained in these pyrolysis experiments are presented in Figure 2. The results correspond to the mean value of two pyrolysis runs, and the deviations were in all cases lower than 0.5%.

It can be observed that an increase in the pyrolysis temperature gives rise to a decrease in the solid fraction and to an increase in the gas fraction. The liquid fraction increases slightly when the temperature is increased from 400 to 550 °C, but remains more or less constant above this temperature. This behaviour is in good agreement with the thermal behaviour of the rope waste observed in the thermobalance, where the main decomposition of the residue was observed to occur below 500 ºC. Similar findings have been reported by other authors working with lignocellulosic wastes (see Table2).

Figure 2

Table2

3.3. The solid carbonaceous residue

The char residue varied from 30 to 21 % at 400 and 800 ºC, respectively. The relatively low yield obtained for the char was somewhat expected for lignocellulosic precursor with a low content of lignin and high content of carbohydrates (high cellulose content). Moreover, these values are also characteristic of lignocellulosic materials containing high methoxyl group contents (hardwood or syringyl lignins) [23].

Some of the chemical properties of the chars obtained at different temperatures are summarized in Table 1. Data suggests that despite the thermal decomposition of the residue seemed to occur mostly below 500 ºC, the pyrolysis reaction does not seem to be complete as the corresponding char (sample C-550) still presents some volatile matter in its carbonaceous structure (i.e., 12.8 wt.%). In fact, the volatile matter decreased gradually when the pyrolysis temperature was raised (carbon content increased), indicating that devolatilization continues (although slowed down) at higher temperatures. Similar findings have been reported for the carbonization of coal and other biomass-derived wastes [23,27,28].

Pyrolysis of the rope waste rendered a carbonaceous material with low ash content. As that the pyrolysis temperature favours the devolatilization of the sample, as it was discussed in paragraph 3.1(thermal profiles) and evidenced by elemental analysis, the overall composition of the solid residue (carbonaceous and inorganic matter) varies with

temperature due to the modification in the volatiles content which is evolved at the different temperatures. Consequently the weight ratio of both the carbon and inorganic matter increases with the pyrolysis temperature. The relatively high amount of heteroatoms, particularly oxygen, in the low temperature samples (C-400 and C-550) indicates that the solid carbonaceous char has abundant functionalities, and confirms that the char still undergoes some pyrolytic reactions when treated above 550 ºC. The textural characterization of the chars obtained at different temperatures (Figure 3) also showed that there is a certain development of microporosity during pyrolysis, being more important as the pyrolysis temperature was raised. Consequently, the solid residue obtained from the pyrolytic degradation of rope wastes could be a potential precursor to be used in the synthesis of low cost adsorbents. Indeed, previous results carried out in our research group have reported the synthesis of high surface carbon adsorbents from this char [7]. The resulting porous carbon also presented outstanding properties as support of metallic species with catalytic applications; the obtained metal-doped carbon supports showing good dispersion of the metal species on the carbon matrix.

The char treated at 400ºC showed a poor porous development compared to the rest of the samples; this suggests that this temperature is too low for a complete degradation of the rope waste, thus inhibiting the evolution of volatiles and the creation of porosity. The porosity of the chars obtained at higher temperatures is more developed, as it can be seen in the CO2 adsorption isotherms (Figure 3), particularly for the samples prepared at 700 and 800ºC. This confirms that even if the main degradation occurs at 550 ºC, there is still a fraction of volatiles decomposing at higher temperatures and creating pores. Moreover, the XRD pattern of the char (Figure 1A) demonstrates that the crystal structure of cellulose is deteriorated during pyrolysis, as the characteristic broad bands of carbon materials due to reflection of (101) and (002) planes are evident at 25 and 44 2θ º, respectively, after the pyrolysis.

Figure 3

3.4. The liquid fraction

The liquid fraction corresponding to condensable vapours obtained during the pyrolysis was recovered and analyzed by GC-MS after separation from the aqueous fraction (mostly water). The chromatogram corresponding to the soluble fraction in dichloromethane from the oil obtained by pyrolysis at 550 ºC of the studied waste is shown in Figure 4, as an example. The pyrograms of the tars obtained at different pyrolysis temperatures rendered similar composition (not shown) with slight variation in the relative abundance of the pyrolysis components.

Figure 4

The pyrolysis products identified in the oil fraction are a complex mixture of carbohydrates and methoxylated phenols that correspond to the different lignin monomers (*p*-hydroxylphenylpropanoid, guaiacylpropanoid and syringylpropanoid lignin units). The main lignin-derived compounds detected were guaiacol, syringol, vanillic acid, eugenol and propenylsyringol. Some products arising from pyrolysis of carbohydrates can be also identified, including: furfural, cyclopentadienone, 2-furaldehyde, and 2-furanmethanol. The complete list of identified products has been included in Table 3. The relative abundance of the individual compounds is shown in Figure 5, and corresponds to the identification of *ca.* 80 % of the chromatographied material (total area). In all cases a predominance of hydrocarbons over phenolic compounds was obtained, which is in good agreement with other studies reported in the literature for lignocellulosic materials.

Table 3

Figure 5

It is interesting to remark that the liquid fraction is rich in flavoring compounds commonly used in food preparation industry. For instance, syringol is the main chemical responsible for the smoky aroma; guaiacol contributes mainly to taste and it is also used as antipyretic

[26]; vanillic acid used as food blending agent, fragrance for perfumes and in pharmaceuticals. Also large quantities of furfural and furfuryl alcohol are obtained, which are known valuable chemicals with industrial applications in synthetic chemistry, refining of lubricating oils, purification of hydrocarbons, or reactive solvents. The acidity of the pyrolysis oil fraction was low (low content of propionic, pentanoic acids), which makes it suitable for further processing for chemical production.

The results show that when pyrolysis is carried out at lower temperatures, the oil fraction was richer in volatile compounds comprising non-aromatic alcohols and ketones, and furans. Moreover, the lignin to hydrocarbons ratio (L/HC) slightly increased as the pyrolysis temperature was raised from 550 to 800 ºC (ratio 0.53 and 0.66, respectively), thus confirming the occurrence of secondary reactions of hydrocarbons at high temperatures. This is also in good agreement with previous observations based on the thermogravimetric analysis. Indeed, although degradation of the rope waste mostly occurred at low temperature, further heating seems to provoke the evolution of medium and high molecular mass volatile compounds arising from the thermal breakdown of the lignin units.

3.5. The gas fraction

Analyses of the composition of the gas fraction obtained from the pyrolysis at various temperatures have shown that CO_2, CO, H_2, O_2, and C_xH_y are the main components released. The histograms in Figure 6 show that CO and CO_2 are the dominant species at all temperatures, followed by methane and H_2. As expected, increasing the pyrolysis temperature lead to a decrease in the amount of CO_2, along with an increase in CO, and H_2 over the whole range of temperatures studied. The concentration of combustible gases changed with the pyrolysis temperature, with a maximum in the yield of the hydrocarbons usually at temperatures higher than 700 °C. This is the case, for instance of methane, which originates from the methoxy groups in the side chains of the lignin units of the ropes, reaching a maximum yield of *ca.* 16 wt.% in the gas fraction when the pyrolysis is carried out at 700 ºC. Traces of benzene, cathecol and phenols were also detected in the gas phase, which are typical products from lignin thermal degradation [29,30].

Figure 6

4. CONCLUSIONS

This work described the characterization of the different fractions obtained from the pyrolysis of lignocellulosic wastes from the rope industry. The pyrolytic reaction of the rope waste started from 250 ºC, showing two decomposition peaks between 300-350 ºC assigned to the depolymerization of hemicelluloses and the decomposition of cellulose oligomers into tars. Above 400 ºC, some degradation still takes place to a small extent, due to the decomposition of cyclic rings and further carbonization of the formed tars.

The oil fraction was the most abundant during the pyrolysis of the rope waste, regardless the temperature, with solid and gas yields varying between 20-30 wt.%. The pyrolysis gases are mainly composed of CO and CO_2, with significant proportions of CH_4 when the pyrolysis is carried out above 600 ºC. A low content of hydrocarbons C2-C4 was also detected.

The GC-MS analysis of the degradation products in the liquid fraction revealed that the bio-oil fraction was rich in flavoring compounds and other valuable chemicals such as furfural, which have large applications in synthetic chemistry, food industry, and pharmaceuticals. The possibility of the recovery of these valuable chemicals, along with the reduced acidity of the pyrolysis oil fraction makes it suitable for further processing in chemical production.

The solid carbonaceous char also displayed interesting features to be used as precursor in the synthesis of low cost high performance porous adsorbents and catalysts supports. The yield of the solid fraction can be modulated by the pyrolysis temperature, which also defines the surface chemistry of the final char residue, and therefore its reactivity. The great potentiality of the solid fraction for the preparation of high surface area carbon adsorbents and supports of metallic particles has been demonstrated in previous works.

Acknowledgements

The autors thank the financial support of the Spanish MICINN (project CTM2008/01956 CTM2011/23378), Acción Integrada AIB2010PT-00209, Acção Integrada Luso-Espanhola 2011 (nº E-11/11). MH thanks CSIC for a postdoctoral contract, and MA and ASM thank FCT for a PhD grant (SFRH/BD/71673/2010) and AdI for a postdoctoral grant (QREN-5523-Watercork), respectively. Finally, Cordex is kindly acknowledged for providing the rope residues.

REFERENCES

[1] Y. Li, Y.W. Mai, L. Ye, Sisal fiber and its composites: a review of recent developments, Compos. Sci. Technol., 60 (2000) 2037-2055.

[2] FAO, Jute, Kenaf, Sisal, Abaca, Coir and Allied Fibres, Statistics, June 2009. Food and Agricultural organization of The United Nations, Rome, pp. 34-38. http://www.fao.org/es/esc/common/ecg/323/en/STAT_BULL_2009.pdf Accessed on October 7th 2011.

[3] A.C.H. Barreto, D.S. Rosa, P.B.A. Fechine, S.E. Mazzeto, Properties of sisal fibers treated by alkali solution and their application into cardanol-based biocomposties, Composites: Part A, 42 (2011) 492-500.

[4] S. Chen, J. Liu, H. Zeng, Structure and antibacterial activity of silver-supporting activated carbon fibers, J. Mater. Sci., 40 (2005) 6223-6231.

[5] R. Fu, L. Liu, W. Huang, P. Sun, Studies on the structure of activated carbon fibers activated by phosphoric acid, J. Appl. Polym. Sci. 87 (2003) 2253-2261.

[6] R. Fu, H. Zeng, Y. Lu, S. Y. Lai, W. H. Chan, C.F. Ng, The reduction of Pt (IV) with activated carbon fibers – an XPS study, Carbon 33 (1995) 657-661.

[7] M. Haro, V. Ruiz, M. Andrade, A.S. Mestre, J.B. Parra, A.P. Carvalho, C.O. Ania, Dual role of copper on the reactivity of activated carbons from coal and lignocellulosic precursors, Microp. Mesop. Mat. (2011) doi:10.1016/j.micromeso.2011.07.005.

[8] A.S. Mestre, Ana S. Bexiga, Margarida Proença, Marta Andrade, Moisés L. Pinto, Inês Matos, Isabel M. Fonseca, Ana P. Carvalho, Activated carbons from sisal waste by chemical activation with K_2CO_3: Kinetics of paracetamol and ibuprofen removal from aqueous solution, Bioresour. Technol. 102 (2011) 8253-8260.

[9] O. Faix, D. Meier, I. Fortman, Studies on isolated lignins and lignins in woody materials by pyrolysis-gas chromatrography-mass spectrometry and off-line pyrolysis-gas chromatography with flame ionization detection, J. Anal. Appl. Pyrol. 11 (1987) 403-416.

[10] J. Ralph, R.D. Hatfield, Pyrolysis-GC-MS characterization of forage materials, J. Agric. Food Chem. 39 (1991) 1426-1437.

[11] J.C. del Rio, A. Gutierrez, A.T. Martınez, Identifying acetylated lignin units in non-wood fibers using pyrolysis-gas chromatography/mass spectrometry, Rapid Commun. Mass Spectrom. 18 (2004) 1181–1185.

[12] J.C. del Rio, A. Speranza, M.J. Gutierrez, A.T. Martinez, Lignin attack during eucalypt wood decay by selected basidiomycetes: a Py-GC/MS study, J. Anal. Appl. Pyrol. 64 (2002) 421–431.

[13] F. Rouquerol, J. Rouquerol, K. Sing, Adsorption by Powders & Porous Solids, Academic Press, London, 1999.

[14] P. Langan, Y. Nishiyama, H. Chanzy, A revised structure and hydrogen-bonding system in cellulose II from a neutron fiber diffraction an alysis, J. Am. Chem. Soc. 121 (1999) 9940-9946.

[15] R. Teeaar, R. Serlmaa, T Paakkari, Crystallinity of cellulose, as determined by CP/MAS NMR and XRD methods, Polymer Bulletin 17 (1987) 231-237.

[16] A. Alemdar, M. Sain, Biocomposites from wheat straw nanofibers: morphology, thermal and mechanical properties Compos. Sci. Technol. 68 (2008) 557– 565.

[17] A. Bismarck, A.K. Mohanty, I. Aranberri-Askargorta, S. Czapla, M. Misra, G. Hinrichsen, J. Springer, Surface characterization of natural fibers; surface properties and water up-take behavior of modified sisal and coir fibers, Green Chem. 3 (2001) 100-107.

[18] A.L.F.S. d'Almeida, D.W. Barreto, V. Calado, J.R.M. d'Almeida, Thermal analysis of less common lignocellulose fibers, J. Thermal Anal. And Calorim. 91 (2008) 2, 405–408.

[19] D. Areseneau, Competitive Reactions in the Thermal Decomposition of Cellulose, Canadian J. Chem. 49 (1971) 632-639.

[20] K.C.M. Nair, R.P. Kumar, S.C. Schit, K. Ramamurthy, S. Thomas, Rheological behavior of short sisal fiber-reinforced polystyrene composites, Composites Part A. Appl. Sci. Manufacturing 31 (2000) 1231-1240.

[21] A.R. Martin, M.A. Martins, O.R.R.F. da Silva, L.H.C. Mattoso, Studies on the thermal properties of Sisal fibers and its constituents. Thermochim. Acta 506 (2010) 14–19.

[22] C. Albano, J. González, M. Ichazo, D. Kaisera, Thermal stability of blends of polyolefins and sisal fiber, Polym. Degrad. Stabil. 66 (1999) 179-190.

[23] E. Jaka, O. Faix, F. Tilla, Thermal decomposition of milled wood lignins studied by thermogravimetry/mass spectrometry, J. Anal. Appl. Pyrol. 40-41 (1997) 171-186.

[24] D.K. Shen, S. Gu, The mechanism for thermal decomposition of cellulose and its main products, Bioresour. Technol. 100 (2009) 6496–6504.

[25] A. M. Azeez, Dietrich Meier, Jeurgen Odermatt, Thomas Willner, Fast pyrolysis of African and European lignocellulosic biomasses using Py-GC/MS and fluidized bed reactor, Energy Fuels 2010, 24, 2078–2085.

[26] C.S. Avenell, I. Sainz-Diaz, A.J. Griffiths, Solid waste pyrolysis in a pilot scale batch pyrolyser, Fuel 75 (1996) 1167-1174.

[27] M. Inguanzo, A. Domınguez, J.A. Menendez, C.G. Blanco, J.J. Pis, On the pyrolysis of sewage sludge: the influence of pyrolysis conditions on solid, liquid and gas fractions J. Anal. Appl. Pyrolysis 63 (2002) 209–222.

[28] S.S. Alves, J.L. Figueiredo, Pyrolysis kinetics of lignocellulosic materials by multistage isothermal thermogravimetry, J. Anal. Appl. Pyrolysis 13 (1988) 123-134.

[29] S.N. Naik, VV. Goud, PK. Rout, AK. Dalai, Production of first and second generation biofuels: A comprehensive review, Renew. Sust. Energ. Rev. 14 (2010) 578–597.

[30] A.H. Carter, M.D. Lond MD, Antipyretic effects of external applications of guaiacol, The British Medical Journal, 7 (1894).

Tables Captions

Table 1. Main characteristics of the rope waste and the chars obtained at different pyrolysis temperatures.

Table 2. Pyrolysis yield for lignocellulosic wastes and biomass samples.

Table 3. List of main GC-MS detectable compounds in the pyrolysis oils of the rope waste at 550 and 800 ºC (area %).

Table 1.

		Raw residue	**C-400**	**C-550**	**C-700**	**C-800**
Elemental analysis (wt.%, dry ash free basis)	**C**	45.7	83.8	91.0	92.8	94.0
	H	5.9	4.4	2.5	1.3	0.9
	N	0.4	0.7	0.8	1.0	1.0
	S	n.d.	n.d.	n.d.	n.d.	n.d.
	O	48.1	11.1	5.7	4.9	4.1
Proximate analysis (wt.%)	**Moisture**	9.8	1.56	0.98	0.37	0.68
	Ash	1.2	5.3	6.3	6.9	5.7
	Volatile Matter	85.9	27.2	12.8	7.8	7.1

n.d. not detected

Table 2.

Reference	Gas	Oil	Solid	Remarks
This work	28	43	22	Sample C-550
This work	27	41	21	Sample C-800
[18]	n.a	n.a	26–31	Temperature range 100–600 °C; various lignocellulose fibers
[21]	n.a	n.a	19.5	Sisal fiber degradation up to 600 °C
[22]	n.a	n.a	22	Sisal fiber degradation and polymer/sisal composites. Up to 500 °C
[23]	n.a	n.a	26–30	Temperature range 120–850 °C; various heating rates
[24]	20–42	30–72	1–47	Temperature range 430–700 °C; cellulose decomposition
[25]	22.6–27.2	50.6–56.2	10.1–22.8	Lignocellulosic biomass; temperature 450–470 °C; fluidized bed reactor
[26]	52.2–99.6	n.a.	0.4–40	Horse manure, straw, chicken litter (not lignocellulosic)

n.a. not available.

Table 3.

	C-550	C-800
ACIDS		
Propionic acid	0.25	
Pentanoic acid, 2-methyl-	0.39	
2-Propenoic acid, 3-(2-furanyl)-, ethyl ester	0.34	
Heptadecanoic acid, heptadecyl ester		3.23
Propargylacetic acid		0.49
NON AROMATIC ALDEHYDES		
2-Butenal, 2-methyl-, dimethylhydrazone	0.16	
Hexanal, 4,4-dimethyl-	0.22	
Propionaldehyde		1.21
3-Pentenal, 4-methyl		0.43
NON AROMATIC KETONES		
1-hydroxy-2- butanone	1.20	1.19
Cyclopentanone	0.44	0.00
2-Cyclopenten-1-one	0.92	0.84
2-Propanone, 1-(acetyloxy)-	0.53	0.75
2-Cyclopenten-1-one, 2-methyl-	0.77	1.82
1,2-Cyclopentanedione		
γ-butyrolactone	0.54	
2(5H)-Furanone	1.26	
1,2-Cyclopentanedione	2.58	0.81
2,3-Dimethylcyclopent-2-en-1-one	0.26	
3-Hexanone	0.44	
2-Butanone, 1-(acetyloxy)	0.48	0.50
3-Methylcyclopentanone	0.56	
3-hexen-2-one, 3-methyl	0.64	
1,2-Cyclopentanedione, 3-methyl	3.62	3.24
2-Cyclopenten-1-one, 2,3-dimethyl-	0.71	
2,4-dimethylcyclopent-4-ene-1,2dione	0.96	
2-Cyclopenten-1-one, 3-ethyl-2-hydroxy	2.64	2.56
2-Butanone, 4-hydroxy-3,3-dimethyl	0.63	
2-(2,2-dimethylpropylidene)cyclopentane-1,3-dione	0.87	
2-Cyclopenten-1-one, 3-ethyl-2-hydroxy	2.81	
2-Butanone, 4-hydroxy-3,3-dimethyl		1.19
2-(2,2-dimethylpropylidene)cyclopentane-1,3-dione		1.12
7,7-dimethylbicyclo[3.3.0]octan-2-one		0.60
2-Butanone, 1-hydroxy-	1.20	1.19
1,3-Cyclopentanedione, 2-(2,2-dimethylpropylidene)-	0.44	0.00
2-Butanone, 3,3-dimethyl-	0.92	0.84
FURANS		
2-Methoxytetrahydrofuran	0.74	0.58
Furfural	6.63	5.71

2,5-Dimethoxytetrahydrofuran		0.56
2-Furanmethanol		5.43
Furan, tetrahydro-2,5-dimethoxy-	0.74	0.60
Ethanone, 1-(2-furanyl)-	1.31	1.60
2-Furancarboxaldehyde, 5-methyl	2.37	1.46
2(3H)-Furanone, 5-methyl-		0.92
2-Furanmethanol, acetate	0.48	0.33
4,7-Methanoisobenzofuran, octahydro-3a,7a-dimethyl-	2.57	
2(5H)-Furanone		1.34
5-Acetoxymethyl-2-furaldehyde	0.79	0.81
3-Furancarboxylic acid	4.33	
BENZENES		
Toluene	1.02	0.60
Benzene, 1,3-dimethyl-	0.37	0.00
O-Hydroxybiphenyl	5.23	4.09
Benzenemethanol, 3-fluoro-		1.85
LIGNIN DERIVED PHENOLS		
Phenol	0.34	0.88
Phenol, 2-methyl-	0.34	0.40
1,2-Benzenediol, 3-methoxy-	0.81	
2,6-Dimethyl-3-(methoxymethyl)-p-benzoquinone		1.42
Phenol, 4-(3-hydroxy-1-propenyl)- (p-Coumaryl alcohol)		0.55
Phenol, 2-butyl-	1.85	1.60
Benzoic acid, 2,3-dihydroxy-		0.38
Phenol, 4-(2-methylpropyl)-	0.73	0.58
2-Pentanone, 1-(2,4,6-trihydroxyphenyl)	2.39	2.92
GUAIACOLS (methoxy-phenols)		
Phenol, 2-methoxy- (guaiacol)	2.12	1.99
2-Methoxy-4-vinylphenol (vinyl guaiacol)	0.76	0.63
Phenol, 2-methoxy-4-methyl- (methyl guaiacol)	0.73	0.47
Phenol, 2-methoxy-4-(2-propenyl)- (eugenol)	0.17	1.58
Phenol, 2-methoxy-4-propyl- (5-propyl guaiacol)	0.40	
Benzoic acid, 4-hydroxy-3-methoxy- (vanillic acid)	3.01	2.16
Benzeneacetic acid, 4-hydroxy-3-methoxy- (Homovanillic acid)	0.67	0.97
Ethyl vanillin		0.47
Phenol, 5-methoxy-2,3,4-trimethyl-	0.41	1.99
SYRINGOLS (dimethoxy phenol)		
Phenol, 2,6-dimethoxy- (SYRINGOL)	6.82	7.63
Phenol, 2,6-dimethoxy-4-(2-propenyl)- (propenil SYRINGOL)	5.22	4.72
Benzaldehyde, 4-hydroxy-3,5-dimethoxy- (Syringaldehyde)	0.48	0.25
Ethanone, 1-(4-hydroxy-3,5-dimethoxyphenyl)-	0.75	0.31
1-(3,4-Dimethoxyphenyl)-1-ethanol		3.31
OTHERS (alkanes, alkenes, non aromatic ketones)	21.14	20.51

Figure 1

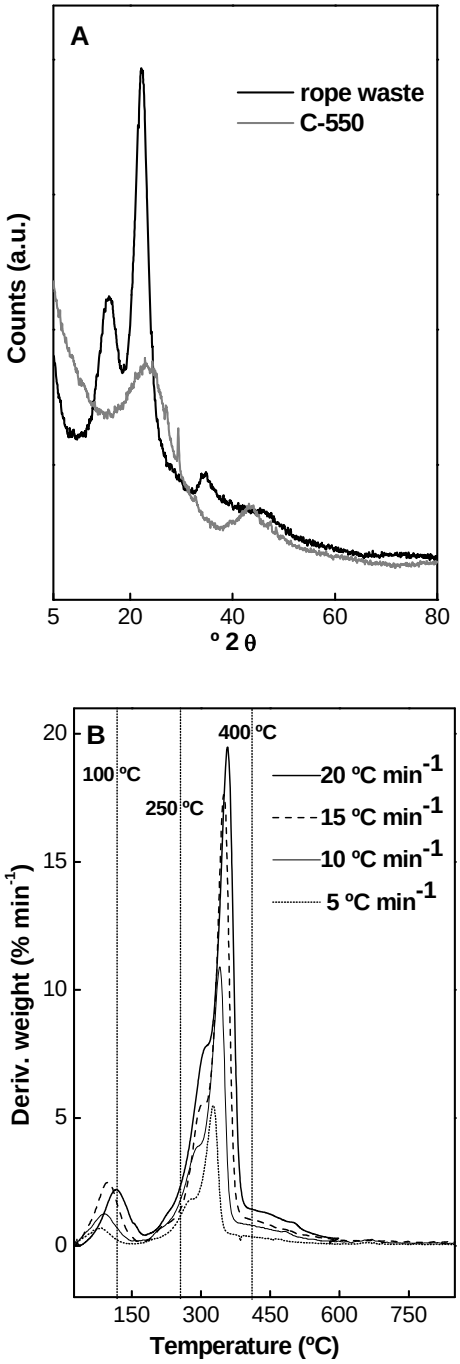
A
rope waste
C-550
Counts (a.u.)
5
20
40
60
80
º 2 θ
B
100 ºC
250 ºC
400 ºC
20 ºC min-1
15 ºC min-1
10 ºC min-1
5 ºC min-1
Deriv. weight (% min-1)
0
5
10
15
20
150
300
450
600
750
Temperature (ºC)

Figure 2

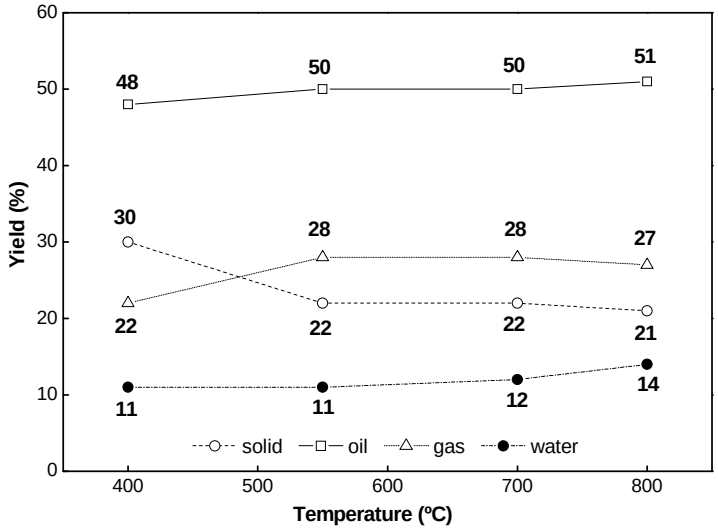

Figure 3

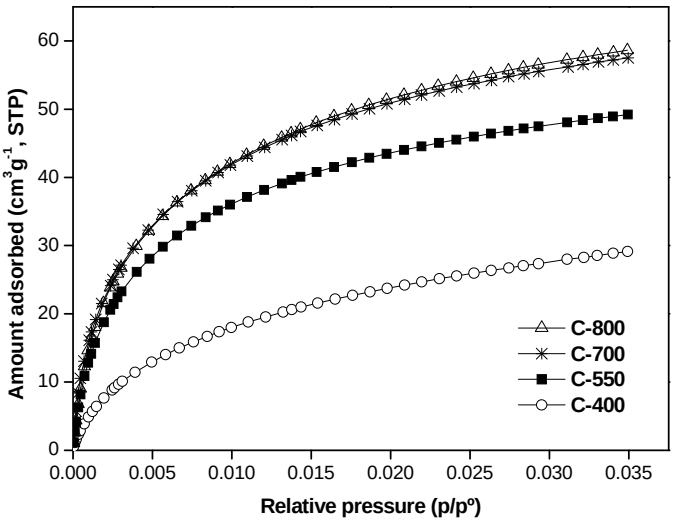

Figure 4

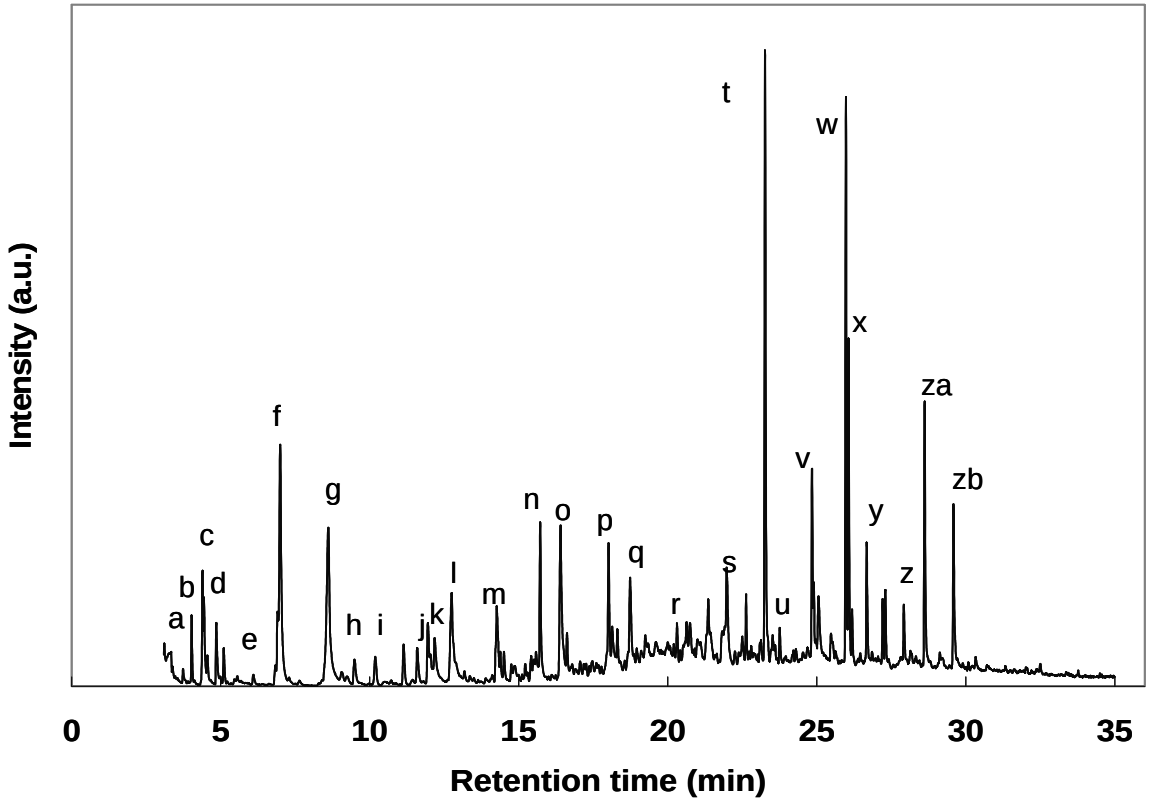
Intensity (a.u.)
Retention time (min)
0
5
10
15
20
25
30
35
a
b
c
d
e
f
g
h
i
j
k
l
m
n
o
p
q
r
s
t
u
v
w
x
y
z
za
zb

Figure 5

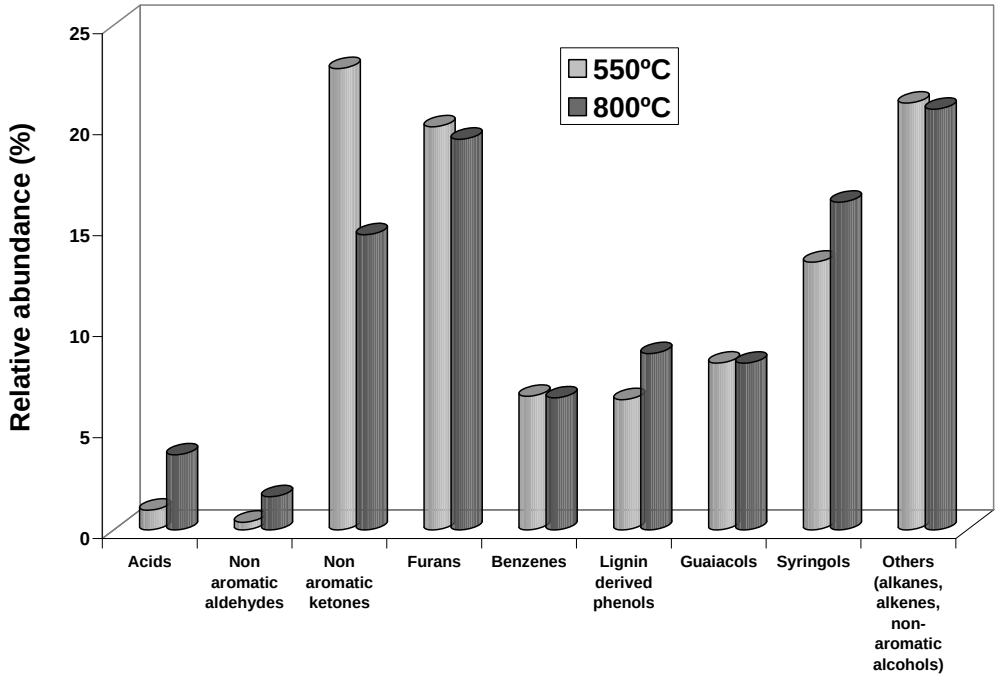
Relative abundance (%)
25
20
15
10
5
0
550ºC
800ºC
Acids
Non aromatic aldehydes
Non aromatic ketones
Furans
Benzenes
Lignin derived phenols
Guaiacols
Syringols
Others (alkanes, alkenes, non-aromatic alcohols)

Figure 6

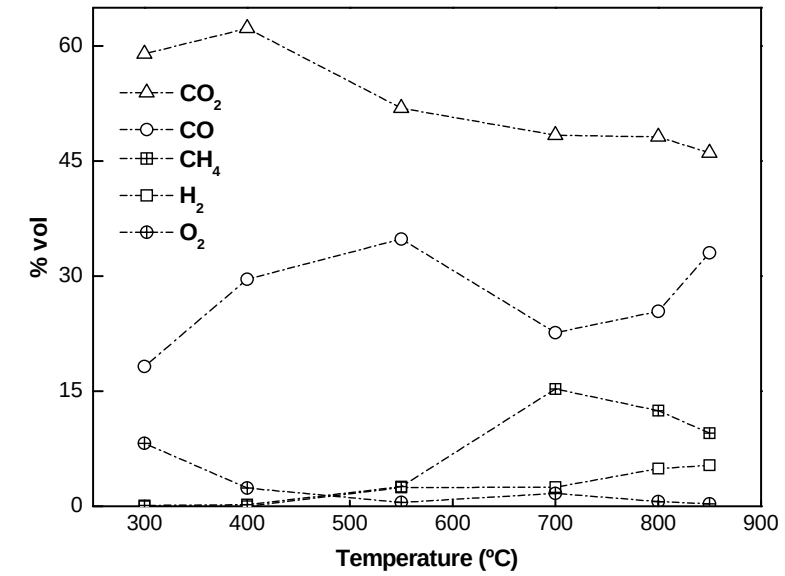
60
45
30
15
0
% vol
CO2
CO
CH4
H2
O2
300
400
500
600
700
800
900
Temperature (ºC)

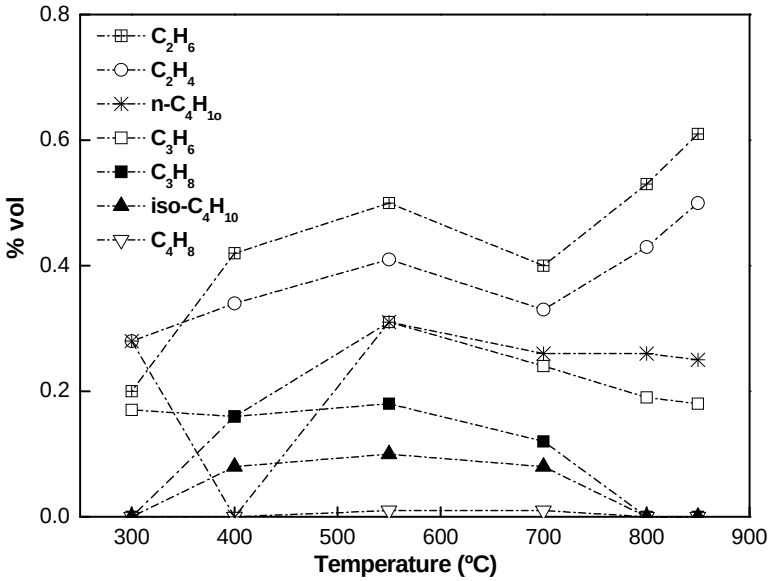
0.8
0.6
0.4
0.2
0.0
% vol
C2H6
C2H4
n-C4H10
C3H6
C3H8
iso-C4H10
C4H8
300
400
500
600
700
800
900
Temperature (ºC)